PHYSICAL REVIEW E **66**, 035203(R) (2002)

Quantum chaos induced by nonadiabatic coupling in wave-packet dynamics

Hisashi Higuchi and Kazuo Takatsuka
Department of Basic Science, Graduate School of Arts and Sciences, The University of Tokyo, 153-8902 Tokyo, Japan
(Received 13 August 2001; revised manuscript received 5 June 2002; published 24 September 2002)

The effect of nonadiabatic coupling due to breakdown of the Born-Oppenheimer approximation on chaos is investigated. A couple of measures (indicators) that detect the extent of chaos in wave-packet dynamics on coupled potential functions are devised. Using them, we show that chaos is indeed induced by a nonadiabatic coupling in individual time-dependent wave-packet dynamics. This chaos is genuinely of quantum nature, since it arises from bifurcation and merging of a wave packet at the quasicrossing region of two coupled potential functions.

DOI: 10.1103/PhysRevE.66.035203 PACS number(s): 05.45.Mt, 03.65.Ge, 82.20.Gk, 34.10.+x

Quantum dynamics on coupled potential functions, in other words, nonadiabatic dynamics [1], which is actually realized in molecular vibrations and chemical reactions, provides a very unique subject in the study of quantum chaos. A total molecular wave function is usually expanded as (we here confine ourselves to a two-state model, and its generalization is trivial) $\Psi(\mathbf{r},\mathbf{R},t)=\phi_1^a(\mathbf{R},t)\Phi_1^a(\mathbf{r};\mathbf{R})+\phi_2^a(\mathbf{R},t)\Phi_2^a(\mathbf{r};\mathbf{R})$, where $\Phi_1^a(\mathbf{r};\mathbf{R})$ and $\Phi_2^a(\mathbf{r};\mathbf{R})$ are the eigenfunctions (with $\mathbf{r}$ the electronic coordinates) of the electronic Hamiltonian given at each nuclear position $\mathbf{R}$. The equations of motion for the nuclear wave functions $\phi_i^a(\mathbf{R},t)$ are given in the following coupled form:

$$i\hbar\frac{\partial}{\partial t}\begin{pmatrix}\phi_1^a\\ \phi_2^a\end{pmatrix}=\begin{pmatrix}T+V_1^a(\mathbf{R}) & X_{12}(\mathbf{R})\\ X_{21}(\mathbf{R}) & T+V_2^a(\mathbf{R})\end{pmatrix}\begin{pmatrix}\phi_1^a\\ \phi_2^a\end{pmatrix}. \quad (1)$$

The Born-Oppenheimer approximation neglects the coupling elements $X_{12}(\mathbf{R})$ and $X_{21}(\mathbf{R})$, and effectively decouples Eq. (1) as

$$i\hbar\frac{\partial}{\partial t}\phi_1^a(\mathbf{R},t)=[T+V_1^a(\mathbf{R})]\phi_1^a(\mathbf{R},t). \quad (2)$$

$V_i^a(\mathbf{R})$ are called the adiabatic potentials. (See, however, Ref. [2] for the conical intersection, in which the coupling is infinite.) Since Eq. (2) has a direct classical counterpart, many studies have been made on the quantum manifestation of the corresponding classical chaos, the so-called quantum chaology [3–5]. In reality, however, the nuclear wave packets in Eq. (1) can bifurcate and merge among themselves due to the coupling elements, thereby bringing about a complicated remixing of quantum waves. The manner of such remixing can depend on the types of nonadiabatic coupling [2]. The pioneering work on chaos due to nonadiabatic coupling has been made by Cederbaum and his co-workers, who were actually studying the dynamics associated with the conical intersections in the vibronic coupling of NO_2, $C_2H_4^+$, and other molecules [2,6]. Heller also investigated randomness induced by semiclassical hopping of trajectories among the relevant diabatic potential functions [7]. It is thus established that the nonadiabatic transition can induce chaos, which has no naive classical counterpart.

The coupled Schrödinger equations similar to Eq. (1) appear also in different studies of physics; the interaction of electron spin with an oscillating electric field described in terms of the spin-boson Hamiltonian [8–10], the quantum mechanical entanglement among composite subsystems [11,12], and so on.

An essential analysis on the mechanism of chaos in nonadiabatic systems of the conical intersection has been made by Leitner *et al.* [13]. Among others, they have shown that the nonadiabatic chaos they studied reflects mostly chaos on the lower one of the corresponding adiabatic potentials, Eq. (2). The latter chaos can readily be induced since the lower adiabatic potential is already highly anharmonic (often of a double-well shape) due to the underlying coupling between the electronic wave functions of different natures. Therefore it is never easy to tell whether the above type of remixing of quantum waves purely causes chaos. Fujisaki and Takatsuka have investigated this particular aspect to show that this can indeed be the case depending on the strength of nonadiabatic coupling and a topographical relation between two adiabatic potential surfaces [14]. The basic strategy was to find a fully chaotic nonadiabatic system that has a regular or weakly chaotic dynamics in the lower adiabatic counterpart. However, their numerical study, and those by Cederbaum and coworkers [2,6,13] as well, resorted to the level statistics of an ensemble of eigenvalues such as the spectral rigidity (Δ_3 statistics) [5,15,16] and the nearest-neighbor level-spacing distribution [5,17]. Here in this report, we show that the nonadiabatic transition can indeed induce chaos in an individual wave-packet dynamics.

The present study is restricted within pure quantum mechanics. As far as quantum chaos on a single potential surface is concerned [Eq. (2)], many sensitive measures (indicators) to detect ''chaos'' have been proposed from many different dynamical aspects [4,5,18–26]. However, these measures are not necessarily suitable to study whether the nonadiabatic interaction itself can cause chaos, simply because they are not so designed. As an illustrative example, let us consider the ''entropy'' for $\phi_1^a(t)$ as $\Omega=-\mathrm{Tr}[|\phi_1^a(t)\rangle\langle\phi_1^a(t)|\ln|\phi_1^a(t)\rangle\langle\phi_1^a(t)|]$, which is time independent and hence one should redefine it as $\hat{\Omega}=-\int d\mathbf{R}|\phi_1^a(\mathbf{R},t)|^2\ln|\phi_1^a(\mathbf{R},t)|^2$ (Ref. [25]). One can naively extend the entropy to the nonadiabatic case of

Eq. (1) as $\Omega_{nad}=-\mathrm{Tr}[|\phi_1^a(t)\rangle\langle\phi_1^a(t)|\ln|\phi_1^a(t)\rangle\langle\phi_1^a(t)|]-\mathrm{Tr}[|\phi_2^a(t)\rangle\langle\phi_2^a(t)|\ln|\phi_2^a(t)\rangle\langle\phi_2^a(t)|]$. But this quantity is already time-dependent in contrast to Ω. (The correct form can be actually constructed, but it is too complicated for numerical application.) Likewise, one can define

$$\hat{\Omega}_{nad}=-\int d\mathbf{R}|\phi_1^a(\mathbf{R},t)|^2\ln|\phi_1^a(\mathbf{R},t)|^2-\int d\mathbf{R}|\phi_2^a(\mathbf{R},t)|^2\ln|\phi_2^a(\mathbf{R},t)|^2.$$

However, this entropy should become larger anyway when a wave packet is bifurcated onto $V_1^a(\mathbf{R})$ and $V_2^a(\mathbf{R})$ irrespective of the presence of chaos. It is therefore quite difficult to determine whether the increment of the entropy is originated from chaos or the nonadiabatic interaction. Similarly, straightforward application of other existing indicators could not necessarily work well. We therefore take this opportunity to reconsider the measure of chaos.

An important property of a classically mixed state is that two phase-space distribution functions, say $\Gamma(t)$ and $\Gamma'(t)$, whose initial distributions $\Gamma(0)$ and $\Gamma'(0)$ are slightly different from each other, are relaxed to a same state irrespective of their initial difference, usually in a manner that $\Gamma(t)-\Gamma'(t)=(\Gamma(0)-\Gamma'(0))\exp(-\alpha t)$. A direct application of the above idea is to calculate a distance between two quantum density operators, $\rho_\mu(t)=|\psi_\mu(t)\rangle\langle\psi_\mu(t)|$ and $\rho_{\mu'}(t)=|\psi_{\mu'}(t)\rangle\langle\psi_{\mu'}(t)|$, where μ and μ' specify the initial conditions of wave packets. A rather general definition of a distance between the two densities is $\mathrm{Tr}(\rho_\mu(t)-\rho_{\mu'}(t))^N$ with an arbitrarily integer N. However, in contrast to the classical exponential decay, one always have $\mathrm{Tr}(\rho_\mu(t)-\rho_{\mu'}(t))^N=\mathrm{Tr}(\rho_\mu(0)-\rho_{\mu'}(0))^N$ for any N. This is due to the quantum coherence arising from Hermiticity of the Hamiltonian. We therefore make the density operators *partly* decoherent. We define local areas A_i $(i=1,2,\ldots)$ in configuration space, which are mutually exclusive, $A_i\cap A_j=\phi$. The projection operator associated with A_i is $P_i=\int_{A_i}dr|r\rangle\langle r|$, with the basic properties $P_iP_j=P_i\delta_{ij}$, $\Sigma_i^{\mathrm{all}}P_i=I$, and $[P_i,H]\neq 0$. A density operator sandwiched by P_i as $\rho_{\mu(i)}(t)=P_i\rho_\mu(t)P_i=P_i|\psi_\mu(t)\rangle\langle\psi_\mu(t)|P_i$ plays a key role as in the theory of Pechukas [22]. $\rho_{\mu(i)}(t)$ may be regarded as a density created by an observation process that is associated with P_i at time t [22]. The norm is well conserved in the modified density, that is, $\Sigma_i\mathrm{Tr}\,\rho_{\mu(i)}=\mathrm{Tr}\,\rho_\mu$. However, at the same time, we should note the fact that $\Sigma_i\mathrm{Tr}\,\rho_{\mu(i)}^N\neq\mathrm{Tr}\,\rho_\mu^N$ for $N\geqslant 2$. Hence, a natural definition of the distance between two partly decoherent density operators is

$$D_0(t)=\sum_{i=1}^{M}S_i^{-2}\mathrm{Tr}[\rho_{\mu(i)}(t)-\rho_{\mu'(i)}(t)]^2, \tag{3}$$

where $S_i=\mathrm{Tr}\,P_i$ is a normalization factor. M is the number of partitioning of the entire space. It is our usual practice to divide the space in such a way that $S_i=S_j$ for all i and j.

One can formulate another simple idea of the distance, which is similar to but different from $D_0(t)$. Let us consider the standard distance between two state vectors in the Hilbert space as $|\langle\psi_\mu(t)-\psi_{\mu'}(t)|\psi_\mu(t)-\psi_{\mu'}(t)\rangle|$. As above, it is quite natural to define the following quantity:

$$D_3(t)=\sum_i S_i^{-2}|\langle\psi_\mu(t)-\psi_{\mu'}(t)|P_i|\psi_\mu(t)-\psi_{\mu'}(t)\rangle|^2, \tag{4}$$

which can measure the relaxation of a wave function in the Hilbert space. $D_3(t)$ retains more information of quantum phase than $D_0(t)$ does. We now test how $D_0(t)$ and $D_3(t)$ work in a single potential dynamics.

The following two-dimensional modified Hénon-Heiles system [27], $H=p_x^2/2m_x+p_y^2/2m_y+(x^2+y^2)/2+x^2(ay^2+y)+y^3(by-1)/3$, is convenient to test the indicators, since its chaotic properties have been well studied. We here set $a=0.6$, $b=0.2$ (see Fig. 1), $m_x=1.0087$, and $m_y=1.0$. An initial wave function is a coherent-state Gaussian wave packet $\psi_\mu(x,y)=N\exp[-(x-x_0)^2/2\hbar+ip_{x0}(x-x_0)/\hbar-(y-y_0)^2/2\hbar+ip_{y0}(y-y_0)/\hbar]$, with $\hbar=0.005$ throughout. We have chosen four sets of the parameters $\mu=(x_0,p_{x0},y_0,p_{y0})$, as listed in Table I, so as to correspond

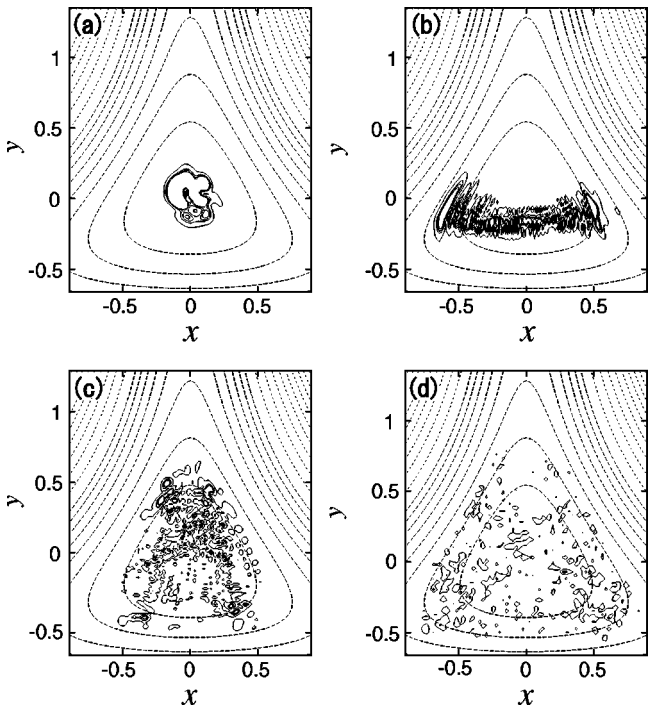

FIG. 1. Wave functions on the modified Hénon-Heiles potential after propagating up to $t=200$. (Absolute units are used throughout.)

TABLE I. Initial locations, momenta, and classical energies characterizing the initial Gaussian wave packets.

	x_0	y_0	p_{x0}	p_{y0}	E_{cl}
(a)	0.1	0.1	0	0	0.010 73
(b)	0	−0.2	0.5066	0	0.15
(c)	0	0.32	0.3594	−0.3	0.15
(d)	0.42	0.425	0	0	0.249 186

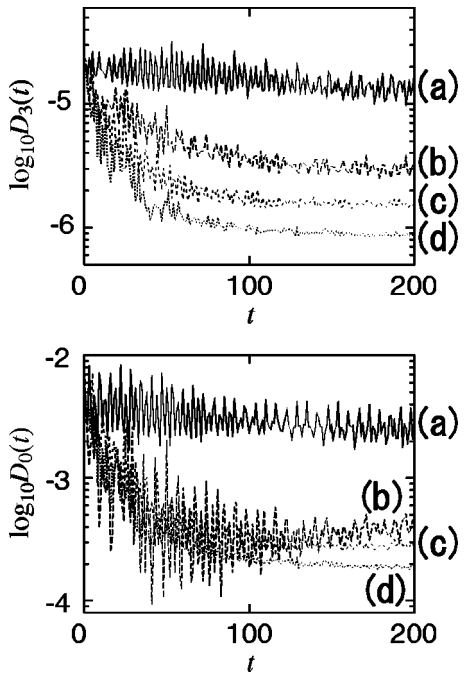

FIG. 2. Chaos on the modified Hénon-Heiles potential function; $\log_{10}D_0(t)$ and $\log_{10}D_3(t)$ in the top and bottom panels, respectively, are plotted versus t. The curves a–d correspond, respectively, to the wave packets a–d in Table I and Fig. 1.

to four typical classical motions, which are (a) highly regular, (b) weakly regular on a torus near the quasiseparatrix, (c) weakly chaotic in a relatively thin quasiseparatrix, and (d) strongly chaotic in a wide chaotic sea. The magnitude of the classical Liapunov exponent should be of the order of (a) $<$ (b) $<$ (c) $<$ (d). Figure 1 displays the snapshots of these four $|\psi_\mu(x,y,t)|^2$ at $t=200$. They clearly display the increasing extent of randomness of the wave packets from the panels (a) to (d). For a given ψ_μ, a slightly different wave packet $\psi_{\mu'}$ is generated by setting $\mu'=(x_0-0.01,p_{x0},y_0,p_{y0})$. Figure 2 shows $D_0(t)$ and $D_3(t)$ for the above packets. As expected, they basically exhibit decaying patterns. Both $D_3(t)$ and $D_0(t)$ show exponential-like decay in the early stage. However, they also bear a large fluctuation, which reflects significant deformation of the wave packets at the turning points. Therefore it would not be a good idea to utilize the exponent in the initial decay as an indicator of chaos. In a later stage, the decay slows down and eventually undergoes saturation, which is a major difference from the classical ergodicity. (Recall that the entropy $\hat{\Omega}$ also shows the similar saturation bounded from above [25,26].) Even if partial decoherence has been introduced through Eqs. (3) and (4), $\psi_\mu(t)$ and $\psi_{\mu'}(t)$ themselves do never coincide with each other. [Recall that $D_3(t)$ and $D_0(t)$ are both time independent for no partition of space ($M=1$).] The present results have been given by the partition number $M=256$ (16 by 16). However, our numerical survey shows that the dependence of $D_0(t)$ and $D_3(t)$ on M is neither very significant nor qualitative for sufficiently large M [28]. It is expected that both $D_3(t)$ and $D_0(t)$ should be bounded from below even for infinitely large partitioning ($M\rightarrow\infty$), unless the wave functions $\psi_\mu(t)$ and $\psi_{\mu'}(t)$ have infinitesimally fine structures (oscillations) in their spatial distributions, which never happens in our generic systems. Anyhow, it turns out that the "converged value" of $D_3(t)$ at a large t ($t\rightarrow\infty$) exhibits a remarkable distinction of their "chaoticity": $D_3(t)$ damps to a smaller value (with a faster speed) for more chaotic wave packet. On the other hand, $D_0(t)$ is found to be not so sensitive as $D_3(t)$ is.

Now we proceed to our goal by extending the above distance $D_0(t)$ for a nonadiabatic system of Eq. (1). Let us write such a vector wave function as $|\psi_\mu\rangle=(|\phi_\mu^{(1)}\rangle\ |\phi_\mu^{(2)}\rangle)^{tr}$, where again μ specifies an initial condition and tr means the transposition. The corresponding density operator is $\rho_\mu=(|\phi_\mu^{(1)}\rangle\ |\phi_\mu^{(2)}\rangle)^{tr}(\langle\phi_\mu^{(1)}|\ \langle\phi_\mu^{(2)}|)$ and the projected density operator is defined as a diagonal matrix $\rho_{\mu(i)}=\mathrm{diag}(P_i|\phi_\mu^{(1)}\rangle\langle\phi_\mu^{(1)}|P_i\ P_i|\phi_\mu^{(2)}\rangle\langle\phi_\mu^{(2)}|P_i)$. Then, $D_0(t)$ is readily extended as

$$D_0(t)=\sum_{i=1}^{M} S_i^{-2}\mathrm{Tr}(\rho_{\mu(i)}-\rho_{\mu'(i)})^2. \tag{5}$$

The extension of $D_3(t)$ is also straightforward, that is,

$$D_3(t)=\sum_i S_i^{-2}\{|\langle\phi_\mu^{(1)}-\phi_{\mu'}^{(1)}|P_i|\phi_\mu^{(1)}-\phi_{\mu'}^{(1)}\rangle|^2 + |\langle\phi_\mu^{(2)}-\phi_{\mu'}^{(2)}|P_i|\phi_\mu^{(2)}-\phi_{\mu'}^{(2)}\rangle|^2\}. \tag{6}$$

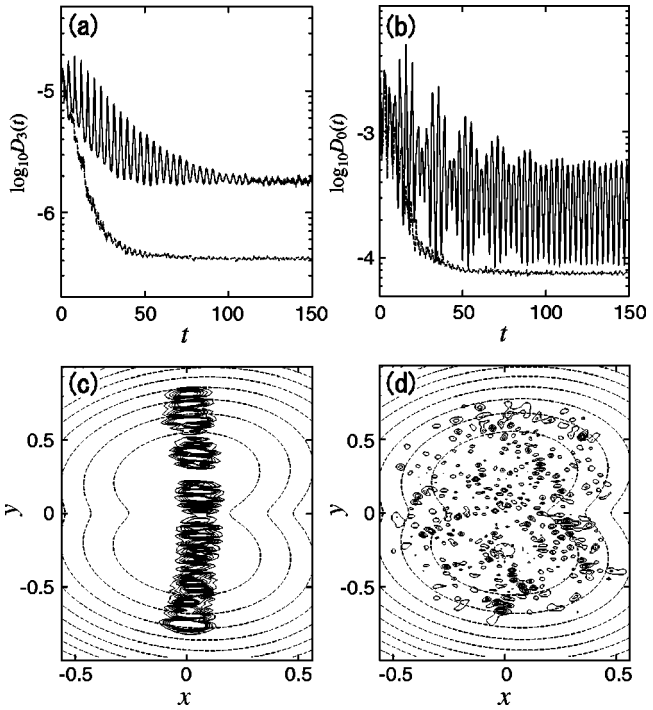

FIG. 3. Quantum chaos induced by the nonadiabatic coupling. (a) $\log_{10}D_3(t)$ versus t. The upper and lower curves arise from the adiabatic and nonadiabatic dynamics, respectively. (b) The same as in the panel (a), but $D_0(t)$ in place of $D_3(t)$. (c) A wave packet on the lower adiabatic potential surface. (d) The lower-part component of the corresponding nonadiabatic wave packet.

We now consider a nonadiabatic problem arising from breakdown of the Born-Oppenheimer approximation. Our investigated system is a simple model system extensively studied by Heller [7], which consists of a pair of two-dimensional harmonic potentials in diabatic representation plus associated coupling elements. These two harmonic potentials make a skew angle θ, which is called the Duschinsky angle. Its Hamiltonian system is $H_{ij}=T\delta_{ij}+V_{ij}^d$ $(i,j=1,2)$, where $T=\frac{1}{2}(p_x^2+p_y^2)$, $V_{ii}^d=\frac{1}{2}(\omega_x^2\xi_i^2+\omega_y^2\eta_i^2)+\epsilon_i$ $(i=1,2)$; with a coordinate transformation $\xi_1=x\cos\theta-(y+y_0)\sin\theta$, $\eta_1=x\sin\theta+(y+y_0)\cos\theta$ and $\xi_2=x\cos\theta+(y-y_0)\sin\theta$, $\eta_2=-x\sin\theta+(y-y_0)\cos\theta$. The off-diagonal elements are assumed to have a form $V_{12}^d=V_{21}^d=f\exp[-\alpha(V_2^d(x,y)-V_1^d(x,y))^2]$, which gives the coupling along the crossing seams. The parameters used are $\omega_x^2=0.872$, $\omega_y^2=1.175$, $\epsilon_2-\epsilon_1=0.001$, $y_0=0.25$, $\theta=\pi/6$, $\alpha=500$, and $f=0.0075$. The relationship between the adiabatic and diabatic representations is in general quite involved, but nonetheless found to be subject to an interesting mathematics of gauge theory [29,30]. In this paper, our ''simulated'' adiabatic potential surfaces are generated by (x,y)-dependent orthogonal transformation of the diabatic potentials V_{ij}^d. The adiabatic potential surfaces $V_1^a(x,y)$ and $V_2^a(x,y)$ are ordered in such a way that $V_1^a(x,y)<V_2^a(x,y)$, and hence $V_1^a(x,y)$ $(V_2^a(x,y))$ is called the lower (upper) adiabatic potential surface. Refer to Fig. 3(c) for $V_1^a(x,y)$.

To see the effect of the nonadiabatic transition, we compare the wave-packet dynamics on the lower adiabatic potential $V_1^a(x,y)$ in Eq. (2) alone and that of the total Hamiltonian in Eq. (1). The relaxation process on $V_1^a(x,y)$ and that in the nonadiabatic system are measured separately with two slightly different wave packets ψ_μ and $\psi_{\mu'}$ in terms of $D_0(t)$ and $D_3(t)$. Figure 3 shows a generic example taken from many calculations. Again, the similar Gaussian wave packet is selected with $\mu=(x_0,p_{x0},y_0,p_{y0})=(0.0,0.0,-0.770\,667,0.0)$. The trajectory on $V_1^a(x,y)$ starting with this initial condition is regular, which has been confirmed using the Poincaré surface of section set at the saddle point. (No naive classical motion exists in the nonadiabatic system.) Figure 3(a) shows $D_3(t)$ for the quantum dynamics on the lower adiabatic potential and that in the nonadiabatic system. The solid curve having the higher value represents the dynamics on $V_1^a(x,y)$, whereas the lower one (broken line) arises from the nonadiabatic system. It clearly evidences that the nonadiabatic interaction applied to $V_1^a(x,y)$ has induced chaos in a significant magnitude. The similar situation is also observed in $D_0(t)$, Fig. 3(b), which turned out to be less sensitive to chaoticity as in Fig. 1. The contour plot of the wave packet on $V_1^a(x,y)$ [Fig. 3(c)] and that on the lower adiabatic surface in the nonadiabatic system [Fig. 3(d)], at $t=150$, visually supports the above conclusion. It is thus confirmed that the nonadiabatic interaction can indeed induce chaos in the level of wave-packet dynamics. More extensive and systematic analyses will be reported in future [28].

The authors thank Dr. H. Fujisaki for valuable discussions.

[1] See H. Nakamura, *Nonadiabatic Transition* (World Scientific, Singapore, 2002) for the latest review.
[2] H. Köppel, W. Domcke, and L.S. Cederbaum, Adv. Chem. Phys. **57**, 59 (1984).
[3] M.V. Berry, Proc. R. Soc. London, Ser. A **413**, 183 (1987).
[4] (a) M. Tabor, *Chaos and Integrability in Nonlinear Dynamics* (Wiley, New York, 1989); (b) F. Haake, *Quantum Signatures of Chaos*, 2nd ed. (Springer, Berlin, 2001).
[5] L.E. Reichl, *The Transition to Chaos* (Springer, Berlin, 1992).
[6] E. Haller, H. Köppel, and L.S. Cederbaum, Chem. Phys. Lett. **101**, 215 (1983).
[7] E.J. Heller, J. Chem. Phys. **92**, 1718 (1990).
[8] R. Graham and M. Höhnerbach, Z. Phys. B: Condens. Matter **57**, 233 (1984).
[9] L. Müller, J. Stolze, H. Leschke, and P. Nagel, Phys. Rev. A **44**, 1022 (1991).
[10] L. Bonci, R. Roncaglia, B.J. West, and P. Grigolini, Phys. Rev. Lett. **67**, 2593 (1991).
[11] A. Tanaka, J. Phys. A **29**, 5475 (1996); Phys. Rev. Lett. **80**, 1414 (1998).
[12] K. Furuya, M.C. Nemes, and G.Q. Pellegrino, Phys. Rev. Lett. **80**, 5524 (1998).
[13] D.M. Leitner, H. Köppel, and L.S. Cederbaum, J. Chem. Phys. **104**, 434 (1996).
[14] H. Fujisaki and K. Takatsuka, Phys. Rev. E **63**, 066221 (2001); see also H. Fujisaki and K. Takatsuka, J. Chem. Phys. **114**, 3497 (2001).
[15] O. Bohigas, M.-J. Giannoni, and C. Schmit, Phys. Rev. Lett. **52**, 1 (1984).
[16] M.V. Berry, Proc. R. Soc. London, Ser. A **400**, 229 (1985).
[17] E.P. Wigner, SIAM Rev. **9**, 1 (1967).
[18] A. Peres, Phys. Rev. A **30**, 1610 (1984).
[19] L. Benet, T.H. Seligman, and H.A. Weidenmüller, Phys. Rev. Lett. **71**, 529 (1993).
[20] L.E. Ballentine and J.P. Zibin, Phys. Rev. A **54**, 3813 (1996).
[21] R. Kosloff and S.A. Rice, J. Chem. Phys. **74**, 1340 (1981); S.A. Rice and R. Kosloff, J. Phys. Chem. **86**, 2153 (1982).
[22] P. Pechukas, J. Phys. Chem. **86**, 2239 (1982).
[23] R. Alicki, D. Makowiec, and W. Miklaszewski, Phys. Rev. Lett. **77**, 838 (1996).
[24] E.J. Heller, J. Chem. Phys. **72**, 1337 (1980).
[25] Y. Ashkenazy, L.P. Horwitz, J. Levitan, M. Lewkowicz, and Y. Rothschild, Phys. Rev. Lett. **75**, 1070 (1995).
[26] N. Hashimoto, Ph.D. dissertation, Nagoya University, Japan, 1996.
[27] N. Hashimoto and K. Takatsuka, J. Chem. Phys. **103**, 6914 (1995).
[28] H. Higuchi and K. Takatsuka (unpublished).
[29] T. Pacher, C.A. Mead, L.S. Cederbaum, and H. Köppel, J. Chem. Phys. **91**, 7057 (1989).
[30] C.A. Mead, Rev. Mod. Phys. **64**, 51 (1992).